specific reciprocal-lattice point can be rotated from point P to point Q by the φ rotation, from Q to R *via* χ, and R to S *via* ω (see Fig. 2.2.6.2).

In the most commonly used setting, the χ plane bisects the incident and diffracted beams at the measuring position. Hence, the vector $\mathbf{d}^*$ lies in the χ plane at the measuring position. However, since it is possible for reflection to take place for any orientation of the reflecting plane rotated about $\mathbf{d}^*$, it is feasible therefore that $\mathbf{d}^*$ can make any arbitrary angle ε with the χ plane. It is conventional to refer to the azimuthal angle ψ of the reflecting plane as the angle of rotation about $\mathbf{d}^*$. It is possible with a ψ scan to keep the *hkl* reflection in the diffraction condition and so to measure the sample absorption surface by monitoring the variation in intensity of this reflection. This ψ scan is achieved by adjustment of the ω, χ, φ angles. When $\chi = \pm 90^\circ$, the ψ scan is simply a φ scan and ε is 0°.

The χ circle is a relatively bulky object whose thickness can inhibit the measurement of diffracted beams at high θ. Also, collision of the χ circle with the collimator or X-ray-tube housing has to be avoided. An alternative is the kappa goniostat geometry. In the kappa diffractometer [for a schematic picture, see Wyckoff (1985, p. 334)], the κ axis is inclined at 50° to the ω axis and can be rotated about the ω axis; the κ axis is an alternative to χ therefore. The φ axis is mounted on the κ axis. In this way, an unobstructed view of the sample is achieved.

2.2.6.3. *Fixed $\chi = 45^\circ$ geometry with area detector*

The geometry with fixed $\chi = 45^\circ$ was introduced by Nicolet and is now fairly common in the field. It consists of an ω axis, a φ axis, and χ fixed at 45°. The rotation axis is the ω axis. In this configuration, it is possible to sample a greater number of independent reflections per degree of rotation (Xuong, Nielsen, Hamlin & Anderson, 1985) because of the generally random nature of any symmetry axis.

An alternative method is to mount the crystal in a precise orientation and to use the φ axis to explore the blind region of the single rotation axis. It is feasible to place the capillary containing the sample in a vertically upright position *via* a 135° bracket mounted on the goniometer head. The bulk of the data is collected with the ω axis coincident with the capillary axis. This setting is beneficial to make the effect of capillary absorption symmetrical. At the end of this run, the blind region whose axis is coincident with the ω axis can be filled in by rotating around the φ axis by 180°. This renders the capillary axis horizontal and a different crystal axis vertical. Hence by rotation about this new crystal axis by $\pm\theta_{\max}$, the blind region can be sampled.

2.2.7. Practical realization of diffraction geometry: sources, optics, and detectors

2.2.7.1. *General*

The tools required for making the necessary measurement of reflection intensities include

(*a*) beam-conditioning items;
(*b*) crystal goniostat;
(*c*) detectors.

In this section, we describe the common configurations for defining precise states of the X-ray beam. The topic of detectors is dealt with in Part 7 (see especially Section 7.1.6). The impact of detector distortions on diffraction geometry is dealt with in Subsection 2.2.7.4.

Within the topic of beam conditioning the following subtopics are dealt with:

– collimation;
– monochromators;
– mirrors.

An exhaustive survey is not given, since a wide range of configurations is feasible. Instead, the commonest arrangements are covered. In addition, conventional X-ray sources are separated from synchrotron X-ray sources. The important difference in the treatment of the two types of source is that on the synchrotron the position and angle of the photon emission from the relativistic charged particles are correlated. One result of this, for example, is that after monochromatization of the synchrotron radiation (SR) the wavelength and angular direction of a photon are correlated.

The angular reflecting range and diffraction-spot size are determined by the physical state of the beam and the sample. *Hence, the idealized situation considered earlier of a point sample and zero-divergence beam will be relaxed.* Moreover, the effects of the detector-imaging characteristics are considered, *i.e.* obliquity, parallax, point-spread factor, and spatial distortions.

2.2.7.2. *Conventional X-ray sources: spectral character, crystal rocking curve, and spot size*

An extended discussion of instrumentation relating to conventional X-ray sources is given in Arndt & Willis (1966) and Arndt & Wonacott (1977). Witz (1969) has reviewed the use of monochromators for conventional X-ray sources.

It is generally the case that the $K\alpha$ line has been used for single-crystal data collection *via* monochromatic methods. The continuum *Bremsstrahlung* radiation is used for Laue photography at the stage of setting crystals.

The emission lines of interest consist of the $K\alpha_1$, $K\alpha_2$ doublet and the $K\beta$ line. The intrinsic spectral width of the $K\alpha_1$, or $K\alpha_2$ line is $\sim 10^{-4}$, their separation $(\delta\lambda/\lambda)$ is 2.5×10^{-3}, and they are of different relative intensity. The $K\beta$ line is eliminated either by use of a suitable metal filter or by a monochromator. A mosaic monochromator such as graphite passes the $K\alpha_1$, $K\alpha_2$ doublet in its entirety. The monochromator passes a certain, if small, component of a harmonic of the $K\alpha_1$, $K\alpha_2$ line extracted from the *Bremsstrahlung*. This latter effect only becomes important in circumstances where the *attenuated* main beam is used for calibration; the process of attenuation enhances the short-wavelength harmonic component to a significant degree. In diffraction experiments, this component is of negligible intensity. The polarization correction is different with and without a monochromator (see Chapter 6.2).

The effect of the doublet components of the $K\alpha$ emission is to cause a peak broadening at high angles. From Bragg's law, the following relationship holds for a given reflection:

$$\delta\theta = \frac{\delta\lambda}{\lambda}\tan\theta. \qquad (2.2.7.1)$$

For proteins where θ is relatively small, the effect of the $K\alpha_1$, $K\alpha_2$ separation is not significant. For small molecules, which diffract to higher resolution, this is a significant effect and has to be accounted for at high angles.

The width of the rocking curve of a crystal reflection is given by (Arndt & Willis, 1966)

$$\Delta = \left\{ \left[\frac{a+f}{s} \right] + \eta + \frac{\delta\lambda}{\lambda}\tan\theta \right\} \qquad (2.2.7.2)$$

when the crystal is fully bathed by the X-ray beam, where a is the crystal size, f the X-ray tube focus size (foreshortened), s the

distance between the X-ray tube focus and the crystal, and η the crystal mosaic spread (Fig. 2.2.7.1).

In the moving-crystal method, Δ is the minimum angle through which the crystal must be rotated, for a given reflection, so that every mosaic block can diffract radiation covering a fixed wavelength band $\delta\lambda$ from every point on the focal spot.

This angle Δ can be controlled to some extent, for the protein case, by collimation. For example, with a collimator entrance slit placed as close to the X-ray tube source and a collimator exit slit placed as close to the sample as possible, the value of $(a+f)/s$ can approximately be replaced by $(a'+f')/s'$, where f' is the entrance-slit size, a' is the exit-slit size, and s' the distance between them. Clearly, for $a' < a$, the whole crystal is no longer bathed by the X-ray beam. In fact, by simply inserting horizontal and vertical adjustable screws at the front and back of the collimator, adjustment to the horizontal and vertical divergence angles can be made. The spot size at the detector can be calculated approximately by multiplying the particular reflection rocking angle Δ by the distance from the sample to the spot on the detector. In the case of a single-counter diffractometer, tails on a diffraction spot can be eliminated by use of a detector collimator.

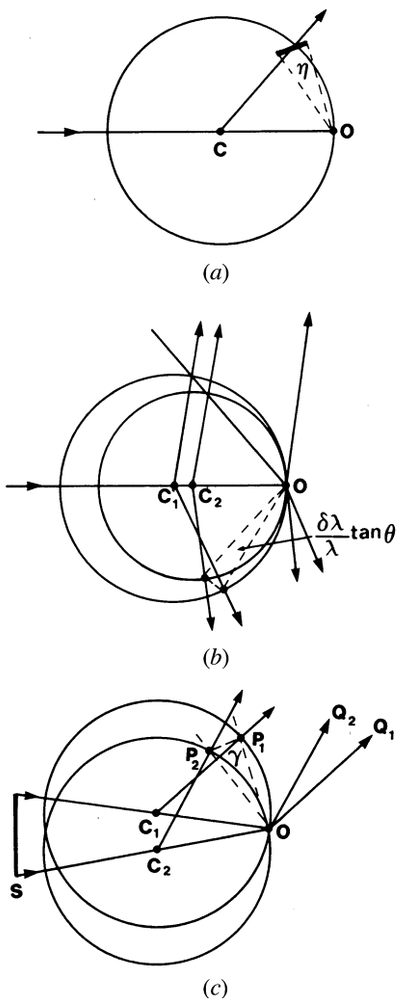

Fig. 2.2.7.1. Reflection rocking width for a conventional X-ray source. From Arndt & Wonacott (1977, p. 7). (*a*) Effect of sample mosaic spread. The relp is replaced by a spherical cap with a centre at the origin of reciprocal space where it subtends an angle η. (*b*) Effect of $(\delta\lambda/\lambda)_{\rm conv}$, the conventional source type spectral spread. (*c*) Effect of a beam divergence angle, γ. The overall reflection rocking width is a combination of these effects.

Spot-to-spot spatial resolution can be enhanced by use of focusing mirrors, which is especially important for large-protein and virus crystallography, where long cell axes occur. The effect is achieved by focusing the beam on the detector, thereby changing a divergence from the source into a convergence to the detector.

In the absence of absorption, at grazing angles, X-rays up to a certain critical energy are reflected. The critical angle θ_c is given by

$$\theta_c = \left[\frac{e^2}{mc^2}\frac{N}{\pi}\right]^{1/2}\lambda, \qquad (2.2.7.3)$$

where N is the number of free electrons per unit volume of the reflecting material. The higher the atomic number of a given material then the larger is θ_c for a given critical wavelength. The product of mirror aperture with reflectivity gives a figure of merit for the mirror as an efficient optical element.

The use of a pair of perpendicular curved mirrors set in the horizontal and vertical planes can focus the X-ray tube source to a small spot at the detector. The angle of the mirror to the incident beam is set to reject the $K\beta$ line (and shorter-wavelength *Bremsstrahlung*). Hence, spectral purity at the sample and diffraction spot size at the detector are improved simultaneously. There is some loss of intensity (and lengthening of exposure time) but the overall signal-to-noise ratio is improved. The primary reason for doing this, however, is to enhance spot-to-spot spatial resolution even with the penalty of the exposure time being lengthened. The rocking width of the sample is not affected in the case of 1:1 focusing (object distance = image distance). Typical values are tube focal-spot size, $f = 0.1$ mm, tube-to-mirror and mirror-to-sample distances ~ 200 mm, convergence angle 2 mrad, and focal-spot size at the detector ~ 0.3 mm.

To summarize, the configurations are

(*a*) beam collimator only;

(*b*) filter + beam collimator;

(*c*) filter + beam collimator + detector collimator (single-counter case);

(*d*) graphite monochromator + beam collimator;

(*e*) pair of focusing mirrors + exit-slit assembly;

(*f*) focusing germanium monochromator + perpendicular focusing mirror + exit-slit assembly.

(*a*) is for Laue mode; (*b*)–(*f*) are for monochromatic mode; (*f*) is a fairly recent development for conventional-source work.

2.2.7.3. *Synchrotron X-ray sources*

In the utilization of synchrotron X-radiation (SR), both Laue and monochromatic modes are important for data collection. The unique geometric and spectral properties of SR renders the treatment of diffraction geometry different from that for a conventional X-ray source. The properties of SR are dealt with in Subsection 4.2.1.5 and elsewhere; see Subject Index. Reviews of instrumentation, methods, and applications of synchrotron radiation in protein crystallography are given by Helliwell (1984, 1992).

(*a*) *Laue geometry: sources, optics, sample reflection bandwidth, and spot size*

Laue geometry involves the use of the fully polychromatic SR spectrum as transmitted through the beryllium window that is used to separate the apparatus from the machine vacuum. There is useful intensity down to a wavelength minimum of $\sim \lambda_c/5$, where λ_c is the critical wavelength of the magnet source. The maximum wavelength is typically ≥ 3 Å; however, if the crystal